Effects of Radiation Tube Head Angulations and Digital Sensor Alignments on Profile Angle Distortion of CAD-CAM Abutments in Periapical Radiography

Choi, Chang-Hun

Department of Dentistry

The Graduate School
Yonsei University

Effects of Radiation Tube Head Angulations and Digital Sensor Alignments on Profile Angle Distortion of CAD-CAM Abutments in Periapical Radiography

Advisor Kim, Sunjai

**A Dissertation Submitted
to the Department of Dentistry
and the Committee on Graduate School
of Yonsei University in Partial Fulfillment of the
Requirements for the Degree of
Doctor of Prosthodontics**

Choi, Chang-Hun

June 2025

Effects of Radiation Tube Head Angulations and Digital Sensor Alignments on Profile Angle Distortion of CAD-CAM Abutments in Periapical Radiography

This Certifies that the Dissertation of Choi, Chang-Hun is approved

Thesis Supervisor	**Kim, Sunjai**
Thesis Committee Member	**Kim, Jee-Hwan**
Thesis Committee Member	**Kim, Jongyub**
Thesis Committee Member	**Park, Ji-Man**
Thesis Committee Member	**Kim, Jong-Eun**

Department of Dentistry
Graduate School
Yonsei University
June 2025

TABLE OF CONTENTS

LIST OF FIGURES

LIST OF TABLES

ABSTRACT

Effects of Radiation Tube Head Angulations and Digital Sensor Alignments on Profile Angle Distortion of CAD-CAM Abutments in Periapical Radiography

Objectives: This study aimed to evaluate the effect of radiographic projection angle deviations—specifically vertical tube head rotation, horizontal tube head rotation, and horizontal sensor rotation—on the accuracy of profile angle measurements in CAD-CAM abutments using periapical radiographs. It also investigated whether the bucco-lingual positioning of the implant on the alveolar ridge affects radiographic distortion.
Materials and Methods: Five implant positions (central, 1.0 mm and 1.5 mm buccal/lingual offsets) were prepared on a mandibular model. Standardized CAD-CAM abutments and monolithic crowns were fabricated. Periapical radiographs were obtained under controlled variations in vertical tube angulation (0°–20°), horizontal tube angulation (mesial/distal, 0°–20°), and horizontal sensor rotation (0°–20°). Interthread distances and mesial/distal profile angles were measured and compared to reference STL data. Crown overlap with adjacent teeth was also assessed.
Results: Vertical angulation over 15° and horizontal sensor rotation over 10° resulted in significant distortion of interthread distance and profile angle. Horizontal tube head rotation caused asymmetrical distortion, particularly in buccally positioned implants. Interthread distance distortion >10% and crown overlap >10% were both associated with profile angle errors exceeding 5°.
Conclusion: Profile angle measurements are highly sensitive to small deviations in projection geometry. Clinicians should aim for perpendicular radiographs with minimal overlap when evaluating CAD-CAM abutments. Interthread distance and crown overlap can serve as useful indirect indicators for radiographic reliability. Further clinical studies are warranted to validate these findings in vivo and explore automated diagnostic tools for improved accuracy.

Keywords: profile angle, CAD-CAM abutment, periapical radiograph, radiation tube rotation, digital sensor rotation

INTRODUCTION

Periapical radiography is one of the primary diagnostic tools used to assess marginal bone loss around dental implants. Due to its cost-effectiveness and convenience, it is commonly employed in clinical practice.[1,2] Despite its advantages, periapical radiographs are limited in that they provide information only on the mesial and distal aspects of implants.[3] Nevertheless, they are considered sufficient for evaluating marginal bone levels in both routine care and research settings.[4,5] Additionally, they play an important role in quantifying changes in marginal bone and enabling early diagnosis of peri-implantitis.[2]

However, periapical radiographs are inherently restricted by their two-dimensional nature, as they project three-dimensional structures onto a flat image.[6] This can result in underestimation of marginal bone loss. One study reported that in cases of peri-implantitis, radiographs underestimated bone loss by an average of 1.3 mm compared to intraoperative measurements.[7]

The primary sources of radiographic error include variations in the X-ray tube head projection angle and sensor plate misalignment.[1,8] These projection errors can occur in both horizontal and vertical directions. Deviations greater than 10° from the ideal angle compromise measurement reliability, while those exceeding 30° result in significant image distortion.[9–11] Large projection angle deviations not only hinder accurate bone level assessment but also impair diagnostic sensitivity and specificity.[2] Sensor misalignment often results from anatomical limitations—such as low palatal vaults in the maxilla or severe resorption in the mandible—which prevent optimal sensor placement.[9,12] Image quality (optimal vs. suboptimal) and inter-examiner variability further contribute to measurement inaccuracies.[13]

Rugani et al. investigated these errors by creating peri-implant defects of varying depths with trephine burs and rotating the X-ray tube head vertically and horizontally to analyze their effects on defect assessment.[14] Their study found that vertical angulation errors significantly increased measurement inaccuracies, while horizontal deviations had

minimal statistical impact. They concluded that vertical angulation consistency is crucial for reliable periapical imaging.

Emerging literature has emphasized the role of prosthesis design—especially the shape of the transgingival portion—in peri-implant tissue health. Katafuchi et al. demonstrated that an emergence angle greater than 30°, as measured between the implant's long axis and the tangent of the prosthetic contour in periapical radiographs, significantly increased the prevalence of peri-implantitis. A convex emergence profile also correlated with higher risk compared to concave or straight profiles.[15] Yi et al. reported similar findings in splinted fixed prostheses, where emergence profile and angle varied by implant position and influenced disease prevalence.[16] Mattheos and Janda further noted that convex emergence profiles with angles over 30° led to increased inflammation and bone loss.[17] A recent systematic review identified overcontoured emergence profiles as a significant risk factor for marginal bone resorption.[18]

With the increased adoption of CAD-CAM abutments—customizable to the implant position, soft tissue thickness, and prosthesis size—emerged new challenges in evaluating their biological impact.[19] Unlike prefabricated conical abutments, CAD-CAM abutments possess unique 3D geometries, making them difficult to assess using traditional radiographic methods. Han et al. introduced the "profile angle" as a refined index to evaluate these contours more effectively.[20] They divided the transmucosal region into three 1-mm intervals from the implant–abutment junction (IAJ) and measured the angle between the implant axis and the abutment’s contour at each level using periapical radiographs.

This profile angle was found to be more predictive of marginal bone loss than the conventional emergence angle.[21] Han’s group reported that the 0–1 mm and 1–2 mm segments significantly correlated with bone loss, while the 2–3 mm segment did not. Nam et al. expanded on these findings by examining subcrestally placed implants and confirming the relationship between profile angle magnitude and marginal bone loss.

Despite the increased clinical use of CAD-CAM abutments, accurate assessment of their profile angles remains a challenge due to radiographic limitations. While implant geometry is standardized and symmetric—allowing for some correction of projection errors—CAD-CAM abutments are highly variable in shape. Even minor deviations in tube head or sensor positioning can cause substantial distortion in the radiographic image.[22] This distortion undermines the reliability of profile angle measurements.

To ensure valid measurements, periapical radiographs must be taken with standardized imaging protocols, minimizing projection angle errors.[2,9,11,23] Although most previous studies on radiographic distortion focused on marginal bone levels or defect depth, the growing clinical emphasis on abutment design necessitates the evaluation of prosthesis contour distortion as well. CAD-CAM abutments, with their pronounced morphological variations near the gingival margin, are particularly susceptible to distortion from minor angular deviations.[24,25] This presents a critical limitation in using periapical radiographs for reliable profile angle analysis.

To date, no study has quantitatively assessed how tube head or sensor rotation affects profile angle measurements in CAD-CAM abutments. Therefore, this study aimed to evaluate the influence of vertical and horizontal tube head angulation and horizontal sensor rotation on profile angle distortion in single-unit implant-supported prostheses restored with CAD-CAM abutments at mandibular first molar sites. We also examined whether implant placement position on the alveolar ridge (centered, buccally, or lingually offset) influences radiographic distortion. The goal was to propose criteria for acceptable clinical error in periapical radiographs used to evaluate profile angles.

MATERIALS AND METHODS

Fabrication of the master model

The right and left first molar of a mandibular acrylic resin model (PRO2002-UL-HD-FEM-28; Nissin Dental, Japan) was removed and the model was scanned using an intraoral scanner (TRIOS3; 3Shape, Denmark) to obtain a STL file. Using a CAD software (Meshmixer; autodesk, USA), and the missing right first molar area was modified to received remobavle dies, then the file was 3D printed using a polyjet-type 3D printer (J5 DentaJet; Stratasys, USA) to fabrticate the master model (Figure 1).

Figure 1) A master model was fabicated. A recipient space was fabricated in the edentulous area to receive 5 different removable dies with implants.

The master model was digitally scanned using an intraoral scanner (TRIOS3), five different implant position groups were designed using an implant planning program (Implant Studio; 3Shape, Denmark) based on a pilot study in which off-center implant positioning (buccal or lingual) led to changes in the measured profile angle. The 5 groups were as follows;

Group B15: Screw hole located 1.5 mm buccally from the central fossa.

Group B10: Screw hole located 1.0 mm buccally from the central fossa.

Group Cent: Implant placed with the screw hole centered on the occlusal central fossa.

Group L10: Screw hole located 1.0 mm lingually from the central fossa.

Group L15: Screw hole located 1.5 mm lingually from the central fossa.

The master model was digitally scanned suing an intraoral scanner (TRIOS3). Based on the planned 5 different implant positions, a fully assisted surgical guides were designed using the same planning program for each implant position and 3D printed using the same 3D printer used for the master model (Figure 2).

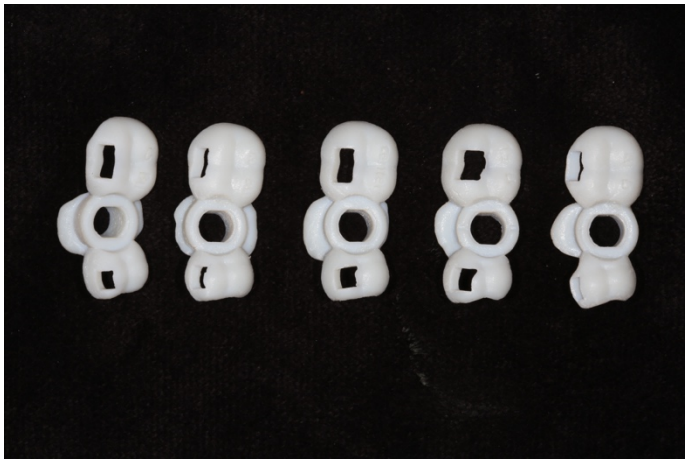

Figure 2) Five surgical guides were 3D printed to position 5 different implant positions.

The recipient site of the master model was lubricated by petroleum jelly, implants were positioned using each surgical guide (Figure 3), then the empty spaced between the implant and the recipient area was fiilled using a self-polymerized acrylic resin (Pattern Resin LS; GC international, USA)

Fugure 3) Implant was located using the surgical guide, using self-polymerizing acrylic resin, removable die with implant was fabricated.

Fabrication of CAD-CAM customized abutments

Regardless of different implant positions, the contour of implant-supported restorations were identical modifying the CAD-CAM abutments. Therefore, 3 different CAD-CAM titanium customized abutments were designed using a CAD program (autoCAD; autodesk, USA). Previous studies measured profile angle in 3 different distance ranges based on the distance from the implant-abutment juction. The distance range 1 (R1) is the 0~1mm range from the implant abutment junction, R2 and R3 were 1~2mm, and 2~3mm, irrespectively. The 3 different CAD-CAM abutments were as follows;

S (symmetrical configuration in bucco-lingual as well as mesio-distal direction) abutment: used for Group Cent. Symmetrical in mesio-distally and bucco-lingualy. In bucco-lingual direction, the profile angles were 15° in R1, 25° in R2, and 60° in R3. In mesio-distal direction, the profile angles were 15°, 25°, and 40° for R1, R2 and R3 (Figure 4A).

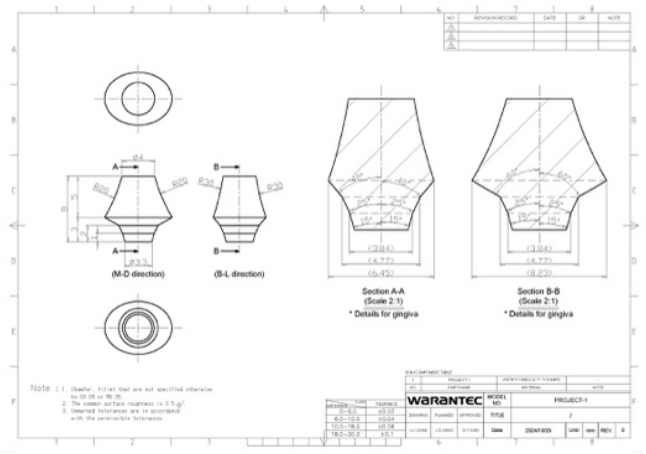

Figure 4A) S abutment.

A10 abutment (asymmetrical configuration in mesio-distal direction, 1.0 mm off-center from central fossa): used for Groups B10 and L10. In mesio-distally off-center side, the profile angles were 15, 25, 60 degree for R1, R2 and R3, whereas 7 degree was applied for R1, R2, and R3 in opposite side. In bucco-lingual direction, the profile angles for each distance ranges were the same to the S abutment (15°, 25°, and 60° for R1, R2 and R3) (Figure 4B).

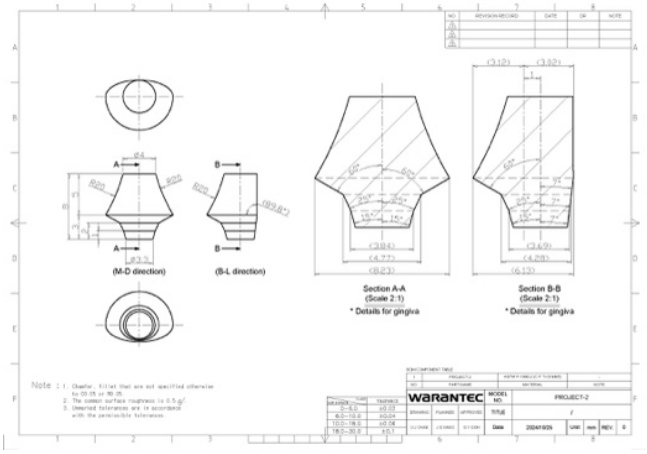

Figure 4B) A10 abutment.

A15 abutment (asymmetrical configuration in mesio-distal direction, 1.5 mm off-center from central fossa): used for Groups B15 and L15. In mesio-distally off-center side, the profile angles were 15, 25, 65 degree for R1, R2 and R3, whereas 0 degree was applied for R1, R2, and R3 in opposite side In bucco-lingual direction, the profile angles for each distance ranges were the same to the S abutment (15°, 25°, and 60° for R1, R2 and R3) (Figure 4C).

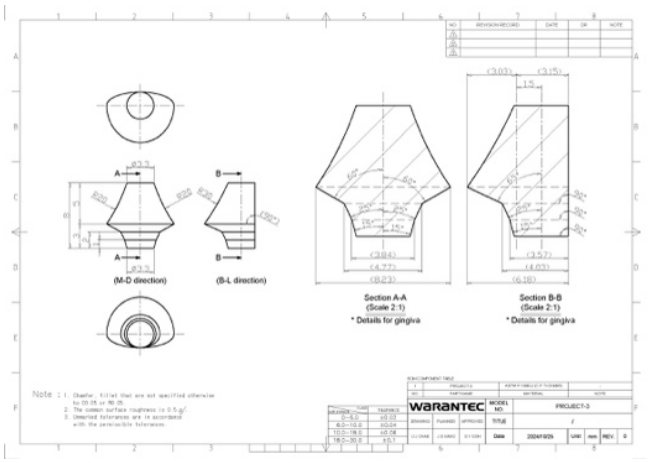

Figure 4C) A15 abutment.

CAD-CAM abutments were fabricated from medical-grade titanium alloy (type VI) using Computer Numeric Control (CNC) milling. Even though, 3 different CAD-CAM abutments have different configuration in mesio-distal direction, the profile angles in bucco-lingual direction were designed identical to standardize the amount of image distortion.

Fabrication of restorations and radiographic jig

The amount of percent overlap between implant and adjacent teeth (restoration) was used to evaluate the amount of distortion by horizontal rotation of radiation tube. The right second premolar and the second molar in the master model were prepared to receive full veneer ceramic crowns, and the master model was digitally scanned using an intraoral

scanner (TRIOS3), and full veneer restorations were designed using a dental CAD program (Cerec inLab20; Dentsply Sirona), then the designed files of restorations were sent to 2-motored 3-axis milling machine (CEREC MC X; Denstply Sirona) to fabricate full veneer lithium disilicate monolithic crowns (IPS e.max CAD; Ivoclar Vivadent). The crowns were cemented onto the abutments using a light-polymerized resin cement (Rely X veneer; 3M, USA). Each implant removable die with a corresponding abutment was positioned into the implant recipeint site of the master model, and digitally scanned to fabricate an implant supported ceramic restoration. All implant restorations were fabicated using the same ceramic material used for the adjacent restorations (Figure 5).

Figure 5) Monolithic lithium disilicate ceramic restorations were luted onto the adjacent abutments.

Figure 6) Three kinds of removable dies with an implant and its corresponding CAD-CAM abutments were placed into the recipient sites. From left to right, Group Cent, Group L10, Group L15.

An implant torque wrench (Torque control device for ratchet 046.049; Straumann, Swiss) was digitally scanned and modified using a CAD program (Meshmixer) to fabricate a custom radiographic jig to standardize the position of radiation tube and the digital sensor.

Radiographic Conditions and Measurements

All periapical radiographs were taken with an intraoral X-ray unit (ProXTM; Planmeca, USA) and digital sensor (RVG 6200; Carestream, USA) under the condition of 70 kV and 1.12 mAs. The variables for radiographic assessments were as follows; 1) the rotation of radiation tube in vertical direction, 2) the rotation of radiation tube in horizontal direction, 3) the rotation of digital sensor in horizontal direction.

1) Rotation of the radiation tube head in vertical direction.

The digital sensor was fixed parallel to the implant axis. The amount of vertical rotation was assiged as 0 degree when the radiation tube was perpendicular to the implant as well as the digital sensor. Then the radiation tube head was rotated in downward-vertical direction by 5° increments were defined as 5°, 10°, 15°, and 20° vertical rotation. The distances between the second and the third threads were measured and profile angle were measured using a CAD program (AutoCAD 2025; Autodesk). Figure 4 is a schematic image of the experimental setting for vertical rotation of radiation tube.

2) Rotation of the digital sensor in horizontal direction

With the X-ray tube head positioned perpendicularly (90°) to the long axis of the implant and both vertical and horizontal angulation was set to 0°, the condition in which the digital sensor was also aligned at 90° to the radiation tube head was defined as 0° horizontal rotation of digital sensor. Radiographs were then taken for all five groups while rotating the digital sensor horizontally in the mesial direction by 5°, 10°, 15°, and 20°. The percent elongation of interthread distance and the profile angles were measured

using a CAD program (AutoCAD 2025). Figure 5 is a schematic image of the experimental setting for vertical rotation of radiation tube (Figure 7).

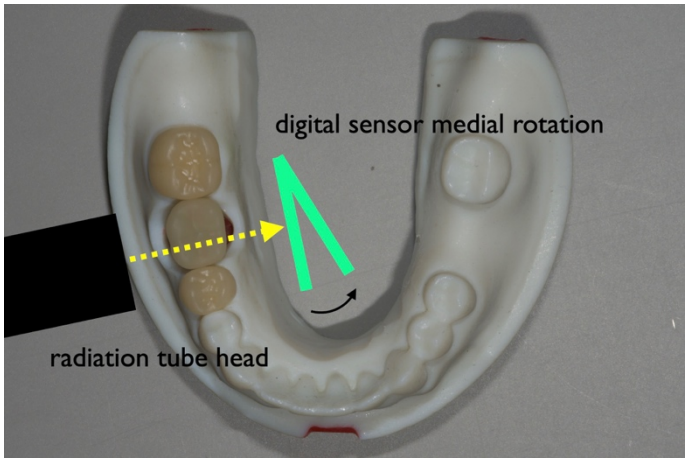

Figure 7) Medial horizontal rotation of digital sensor

3) Rotation of the radiation tube head in horizontal direction.

The digital sensor was set as 0 degree horizontal rotation. Radiation tube head was rotated in distal as well as mesial direction from 0 degree to 5°, 10°, 15°, and 20°. The amount of percent overlap with adjacent tooth restoration was represented as % of implant restoration crown. The mesial and distal profile angle in each distance range was also measured in each rotation environment (Figure 8).

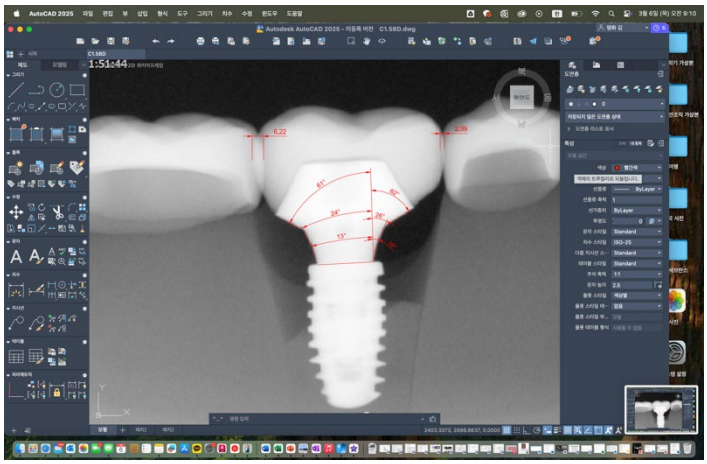

Figure 8) Measurements of the amount of percent overlap between adjacent restorations. The number in distal and mesial overlap was 6.22 and 2.39 irrespectively, in this image (the number is a unit in the CAD program, not the millimeters). The number was divided by the mesio-distal number of implant restoration (105.71 which is not shown in this picture) resulting 5.9% and 2.3% in distal and mesial aspect of the implant restoration. Mesial and distal profile angles were measured in 3 distance ranges, resulting 13°, 24°, 61° in the mesial aspect, and 16°, 26°, 62° in the distal aspect.

All radiographs were taken under consistent settings. Each measurement was repeated twice by a trained evaluator, and the average was used. STL files were analyzed with a CAD program (Meshmixer) to determine baseline profile angles at 0~1 mm, 1~2 mm, and 2~3 mm distance ranges from the implant-abutment junction.

Due to the geometric consistency of the CAD-CAM abutments and controlled radiographic settings, only one measurement values for each radiographic condition was used, therefore, no statistical analysis was performed. Instead, the gross trend of differences were analyzed for the future research.

RESULTS

1. The amount of percent elongation of interthread distance by vertical rotation of radiation tube head.

As the vertical rotation of the radiation tube head increased from 0° to 5°, 10°, 15°, to 20°, the interthread distance gradually increased across all groups. Particularly, when the vertical angulation reached 15°, the increase in interthread distance became more pronounced. The amount of percent elogation was more pronounced in Group B15 and B10 compared to Groups L10 or L15. At 20° of vertical rotation, group B15 resulted 39% elongation whereas group L15 had only 7.9% elongation (Table 1).

Table 1. The amount of elongation of interthread distance by vertical tube angulation (%).

	0	5	10	15	20
B15	7.2	13.2	20.3	26.3	39.0
B10	5.0	8.9	17.0	20.8	22.0
Cent	0.0	5.7	12.7	18.9	20.6
L10	-5.7	-3.8	3.3	9.3	16.7
L15	-16.0	-6.9	-0.7	4.3	7.9

2. The amount of percent elongation of interthread distance by horizontal rotation of digital sensor.

As the amount of rotation increased, interthread distances showed a marked rise (Table 2).

Table 2. The amount of elongation of interthread distance by horizontal digital sensor angulation (%).

	0	5	10	15	20
B15	19.1	52.8	111.3	136.1	
B10	5.7	19.9	91.1	122.6	143.4
Cent	0.0	22.1	89.8	132.1	139.4
L10	15.1	55.5	94.9	128.6	136.4
L15	15.6	24.5	90.3	121.8	134.8

Even when the horizontal rotation of the digital sensor was set to 0°, an increase in interthread distance was observed in Group B15 and Group L15, where the implant was positioned 1.5 mm buccally or lingually from the center of the alveolar ridge, compared to Group Cent, where the implant was centrally positioned. Similar to the previous findings, as the horizontal rotation of the digital sensor increased from 5° to 20°, the B15 group showed a greater increase in interthread distance compared to the L15 group. At 20° of rotation, the distortion in the B15 group was severe enough to preclude accurate measurement.

3. Assessment of crown overlap between adjacent restorations by distal rotation of radiation tube head.

With the sensor fixed at 0° rotation, the tube head was rotated distally in 5° increments, the mesial overlap between the second premolar and the implant restorations, and the distal overlap between the implant restoation and the second molar restorations were presented in Table 3 and Table 4.

Table 3. The amount of overlap between the first premolar and the implant restorations by distal horizontal rotation of radiation tube head (%).

	0	5	10	15	20
B15	1.3	0.0	2.3	5.6	9.7
B10	1.3	0.0	1.7	4.9	9.6
Cent	0.8	0.0	2.8	5.2	9.3
L10	0.0	0.0	2.5	5.8	11.3
L15	1.7	0.0	2.8	4.8	10.0

At 15° horizontal rotation, overlap of about 5% of the mesiodistal crown width was observed. At 20°, approximately 10% overlap was noted in all groups.

Table 4. The amount of overlap between the implant and the second molar restoations by distal horizontal rotation of radiation tube head (%).

	0	5	10	15	20
B15	0.0	3.4	5.9	11.8	15.5
B10	0.0	1.5	3.9	7.7	13.0
Cent	0.0	2.3	4.9	9.7	13.9
L10	0.0	2.3	5.0	9.3	13.5
L15	0.0	2.8	5.9	10.0	15.4

Greater % overlap was observed at the distal aspect of implant restoration (between the implant and the second molar restorations). At 15° rotation, overlap of about 10% was noted, and while 13 to 15 percent overlap was noted when the horizontal rotation was 20 degree.

4. Assessment of crown overlap between adjacent restorations by distal rotation of radiation tube head.

As the radiation tube head was rotated mesially, overlap with the second premolar and second molar increased in all groups (Tables 5 and 6). Unlike distal rotation, mesial rotation resulted in greater overlap on the mesial aspect than the distal aspect.

Table 5. The amount of overlap between the first premolar and the implant restorations by mesial horizontal rotation of radiation tube head (%).

	0	5	10	15	20
B15	3.2	0.9	7.4	11.8	
B10	0.0	3.3	7.6	13.7	
Cent	0.0	3.6	7.1	11.4	13.8
L10	0.0	2.5	7.3	9.1	
L15	0.0	3.3	5.7	10.2	

Table 6. The amount of overlap between the implant and the second molar restoations by distal horizontal rotation of radiation tube head (%).

	0	5	10	15	20
B15	1.7	0.7	4.8	9.6	
B10	0.0	1.5	5.0	10.0	
Cent	1.0	0.0	3.9	7.5	11.7
L10	0.0	1.6	5.2	8.8	
L15	1.1	0.0	1.4	4.8	

5. Profile Angle Measurements

1) Effect of the vertical rotation of radiation tube

Profile angles on mesial and distal aspects were measured as vertical angulation increased (Table 7). A general trend of decreasing profile angle was noted. Seven out of

120 conditions resulted in more than 5 degrees of profile angle differences between measured in radiographs and in STL files at 20° vertical rotation and only one condition at 15° of radiation tube rotation.

Table 7. Measured profile angle as the vertical rotation of radiation tube.

		vertical rotation of radiation tube									
		0	5	10	15	20	0	5	10	15	20
		mesial profile angle					distal profiel angle				
range 0~1	B15	14	13	15	13	12	13	14	15	13	13
	B10	14	13	13	12	14	14	13	13	14	14
	Cent	15	15	15	12	12	14	14	14	15	13
	L10	13	16	14	14	15	13	13	13	11	11
	L15	16	16	14	13	12	11	10	13	13	12
range 1~2	B15	25	23	21	21	18	24	25	24	23	23
	B10	25	24	23	23	22	23	23	23	23	22
	Cent	28	24	26	21	21	24	21	23	21	21
	L10	25	24	23	23	24	23	23	22	22	18
	L15	27	27	25	26	24	21	21	23	22	18
range 2~3	B15	60	61	59	58	55	60	60	59	58	56
	B10	60	60	60	59	58	61	60	60	58	58
	Cent	63	61	63	59	57	57	58	58	56	57
	L10	62	60	59	60	58	59	58	59	58	55
	L15	63	61	61	61	58	57	59	59	58	54

As vertical rotation increased from 5° to 20°, the difference in profile angle compared to the 0° reference progressively increased. On average, the mesial profile angle differences at 5, 10, 15, 20 degree rotation were 1.3°, 1.5°, 2.5°, and 3.6°, while the distal aspects were 0.8°, 0.9°, 1.3°, and 2.1°, respectively.

2) Effect of the horizontal rotation of digital sensor

Similar to the trend observed with increasing vertical rotation, as the digital sensor's horizontal rotation increased from 5° to 20°, the difference in profile angle compared to the 0° reference progressively increased (Table 8). On average, the mesial profile angle differences at 5°, 10°, 15°, and 20° were 0.7°, 1.3°, 1.5°, 2.1° respectively, while the corresponding differences on the distal aspect were 0.8°, 1.2°, 1.0°, 2.1°.

Table 8. Measured profile angles as the medial rotation of digital sensor.

		medial rotation of digital sensor									
		0	5	10	15	20	0	5	10	15	20
		mesial profile angle					distal profiel angle				
range 0~1	B15	14	14	14	15	16	15	14	14	14	16
	B10	14	14	14	15	16	14	13	16	14	18
	Cent	15	14	14	16	16	14	14	14	15	16
	L10	16	13	15	14	16	14	14	14	13	16
	L15	15	14	11	12	11	15	14	13	14	12
range 1~2	B15	23	24	23	25	24	24	23	22	24	25
	B10	25	25	26	26	24	24	25	23	24	25
	Cent	24	23	23	25	24	24	24	24	23	24
	L10	25	25	22	24	22	24	25	23	23	24
	L15	24	23	23	23	22	24	25	25	23	22
range 2~3	B15	61	61	60	63	65	61	61	63	64	66
	B10	60	61	62	63	65	60	59	62	63	66
	Cent	60	60	61	60	60	59	59	58	60	60
	L10	60	60	59	59	59	59	61	61	60	58
	L15	60	59	57	58	55	59	61	58	59	57

3) Effect of horizontal rotation of the radiation tube

(1) Distal Rotation of radiation tube

Profile angle differences greater than 5° were observed only in 3 mesial and 6 distal measurements out of a total of 150 conditions. The maximum difference was 10°, which occurred in the B15 group at 20° of horizontal digital sensor rotation. The average differences were 1.3° on the mesial side and 1.7° on the distal side (Table 9)

Table 9. Measured profile angles by horizontal distal rotation of radiation tube

		horizontal distal rotation of radiation tube									
		0	5	10	15	20	0	5	10	15	20
		mesial profile angle					distal profiel angle				
range 0~1	B15	13	14	16	16	17	12	14	13	12	7
	B10	13	12	12	16	17	13	11	9	10	9
	Cent	12	12	14	16	19	14	13	14	13	11
	L10	15	13	14	16	17	15	12	14	12	11
	L15	12	13	13	15	14	15	15	14	13	13
range 1~2	B15	24	23	26	27	29	24	24	24	21	15
	B10	25	23	24	26	30	25	22	24	22	21
	Cent	23	24	24	27	28	23	23	20	22	25
	L10	25	25	25	24	28	25	23	23	23	22
	L15	25	23	25	24	25	25	25	23	24	23
range 2~3	B15	60	61	62	63	63	61	59	61	61	60
	B10	59	60	61	62	62	60	59	61	60	60
	Cent	61	60	59	60	60	60	61	62	61	60
	L10	61	60	59	60	60	59	60	60	59	59
	L15	59	61	59	60	60	61	60	60	61	60

(2) Mesial Rotation

Profile angle deviations greater than 5° were observed in 4 mesial and 5 distal measurements out of a total of 150 conditions. The maximum deviation, 11°, was found in the B10 group at 20° of rotation. The average differences were 2.1° on the mesial side and 1.9° on the distal side (Table 10).

Table 10. Measured profile angles by horizontal mesial rotation of radiation tube

		horizontal mesial rotation of radiation tube									
		0	5	10	15	20	0	5	10	15	20
		mesial profile angle					distal profiel angle				
range 0~1	B15	13	11	13	11	10	11	15	16	16	19
	B10	14	14	11	13	11	14	16	17	18	25
	Cent	14	13	13	13	13	15	14	15	17	20
	L10	14	13	11	13	12	13	16	17	18	17
	L15	13	13	11	11	12	15	17	18	18	18
range 1~2	B15	24	22	21	21	18	23	26	26	27	29
	B10	22	22	20	21	16	25	26	28	28	31
	Cent	22	25	25	24	23	24	24	27	29	31
	L10	23	23	24	23	25	24	27	27	26	25
	L15	23	23	22	21	24	24	25	27	26	27
range 2~3	B15	61	60	59	60	57	60	61	63	63	65
	B10	59	61	61	62	59	62	61	63	63	64
	Cent	60	60	60	60	62	61	59	60	60	61
	L10	61	60	61	62	63	61	60	62	59	60
	L15	60	61	59	61	62	60	60	61	60	62

DISCUSSION

There has been growing clinical interest in the association between the profile angle of implant restorations using CAD-CAM abutments and the amount of marginal bone loss. Periapical radiographs are commonly used for profile angle measurement and are considered useful tools for evaluating marginal bone levels during routine follow-up.[11,26,27] However, periapical radiographs are inherently limited by their two-dimensional nature, as they project three-dimensional structures onto a flat image, leading to potential inaccuracies in evaluating implant geometry and surrounding anatomical landmarks.[28]

Previous studies assessing profile angles using periapical radiographs have primarily relied on two-dimensional projections of complex three-dimensional CAD-CAM abutments. These studies did not account for angulation deviations that may occur clinically, such as rotation of the tube head or sensor. In practice, despite efforts to obtain radiographs perpendicular to the implant's long axis and avoid overlap with adjacent teeth, ideal imaging conditions are not always achieved. In such cases, inaccurate profile angle measurements may lead to erroneous conclusions regarding the relationship between abutment shape and marginal bone loss.

This study aimed to identify three key sources of error that may affect profile angle measurements in clinical radiography: horizontal tube head rotation, vertical tube head rotation, and horizontal sensor rotation. Furthermore, we investigated whether the bucco-lingual positioning of implants on the alveolar ridge could influence profile angle distortions in periapical imaging. It is important to note that measuring profile angles is inherently different from assessing marginal bone level or defect depth. Rugani et al. examined the effect of vertical and horizontal tube angulation on the radiographic evaluation of peri-implant bone defects.[12] While vertical angulation led to statistically significant errors, horizontal angulation had minimal impact. However, the bone defects in that study were symmetrical and circumferential, created with trephine drills, which are structurally different from the asymmetrical, freeform geometry of CAD-CAM abutments.

Our results showed that both vertical and horizontal tube head rotation significantly influenced profile angle measurements. Increased vertical angulation tended to reduce measured profile angles, while increased horizontal angulation generally led to overestimation. These findings suggest that profile angle measurements are more sensitive to angulation errors than marginal bone level assessments, and thus require greater attention to radiographic positioning. An interesting finding of this study was that implants positioned more buccally exhibited greater interthread distance distortion when subjected to tube head or sensor rotation, compared to those placed lingually. This is likely due to the buccal implant being closer to the X-ray source, thereby amplifying distortion effects. Although vertical tube head rotation of 20° significantly altered profile angles across all groups, there was no consistent difference in distortion between buccally and lingually placed implants, except in a few specific ranges (e.g., R2 mesial angles).

Overall, vertical rotation greater than 15° frequently resulted in profile angle measurement errors exceeding 5°. Clinically, when interthread distance distortion exceeds 10%, especially in non-lingual implant positions, re-imaging should be considered to obtain reliable profile angle data. In contrast, horizontal tube head rotation had a more pronounced impact on profile angles. Distal rotation increased mesial angles and decreased distal ones, while mesial rotation produced the opposite effect. These changes were more severe in buccally positioned implants compared to lingually positioned ones. This finding implies that horizontal angulation introduces asymmetrical distortion in mesial vs. distal profile angle measurements and that buccally positioned implants are more susceptible. When crown overlap with adjacent teeth exceeds 5%, there is a higher likelihood of profile angle overestimation, reinforcing the need for image retakes in such scenarios.

Based on these findings, we propose two quantitative indicators to estimate the reliability of profile angle measurements. First, interthread distance distortion exceeding 10% suggests vertical angulation greater than 15°, which likely leads to underestimation of the profile angle. Second, crown overlap exceeding 10% of the implant restoration’s

width indicates horizontal angulation greater than 15°, which may result in exaggerated profile angles. In both cases, image retakes are recommended. Lastly, the implant's position on the alveolar ridge affects its sensitivity to distortion from horizontal angulation. Buccally positioned implants are more prone to measurement error than lingually positioned ones under the same conditions. Thus, if overlap with adjacent restorations exceeds minimal levels, especially on the buccal side, radiographic re-acquisition is advised.

Future studies should include a larger number of radiographic images under various conditions to allow for robust statistical analysis and to better define clinically acceptable thresholds. The development of automated radiographic analysis tools for profile angle measurement may also enhance standardization and minimize operator-dependent variability. Further, future studies build upon these findings by incorporating patient-specific anatomical variations, validating results in clinical settings, and investigating whether three-dimensional imaging modalities (such as CBCT with metal artifact reduction) provide improved accuracy for profile angle assessment.

The current study demonstrated that unlike marginal bone level assessment, profile angle measurements in CAD-CAM abutments are highly sensitive to radiographic projection errors, such as vertical and horizontal tube head rotation and horizontal sensor misalignment. Among these, horizontal tube head angulation exerted the greatest impact, especially in buccally positioned implants. Vertical angulations exceeding 15° and horizontal sensor rotations over 10° led to measurable distortion in both interthread distance and profile angle. Furthermore, crown overlap greater than 10% with adjacent teeth was associated with significant overestimation of the profile angle.

Based on the results of the current study, two practical indicators can be used to evaluate the reliability of profile angle measurements on periapical radiographs. First, if the interthread distance appears distorted by more than 10% compared to the known implant dimensions, this may indicate an error in vertical angulation. Second, if the implant crown overlaps the adjacent tooth by more than 10% of its width, it likely reflects

a horizontal projection error. In either situation, it is advisable to retake the radiograph to ensure an accurate and reliable assessment of profile angles.

References

1. Vadiati Saberi B, Khosravifard N, Ghandari F, Hadinezhad A. Detection of peri-implant bone defects using cone-beam computed tomography and digital periapical radiography with parallel and oblique projection. *Imaging Sci Dent* 2019;49:265-272.
2. Galindo-Moreno P, Catena A, Pérez-Sayáns M, Fernández-Barbero JE, O'Valle F, Padial-Molina M. Early marginal bone loss around dental implants to define success in implant dentistry: A retrospective study. *Clin Implant Dent Relat Res* 2022;24:630-642.
3. Ritter L, Elger MC, Rothamel D, et al. Accuracy of peri-implant bone evaluation using cone beam CT, digital intra-oral radiographs and histology. *Dentomaxillofac Radiol* 2014;43:20130088.
4. Derks J, Tomasi C. Peri-implant health and disease. A systematic review of current epidemiology. *J Clin Periodontol* 2015;42 Suppl 16:S158-171.
5. Lang NP, Berglundh T. Periimplant diseases: where are we now?--Consensus of the Seventh European Workshop on Periodontology. *J Clin Periodontol* 2011;38 Suppl 11:178-181.
6. Tyndall DA, Brooks SL. Selection criteria for dental implant site imaging: a position paper of the American Academy of Oral and Maxillofacial radiology. *Oral Surg Oral Med Oral Pathol Oral Radiol Endod* 2000;89:630-637.
7. García-García M, Mir-Mari J, Benic GI, Figueiredo R, Valmaseda-Castellón E. Accuracy of periapical radiography in assessing bone level in implants affected by peri-implantitis: a cross-sectional study. *J Clin Periodontol* 2016;43:85-91.
8. Eickholz P, Kim TS, Benn DK, Staehle HJ. Validity of radiographic measurement of interproximal bone loss. *Oral Surg Oral Med Oral Pathol Oral Radiol Endod* 1998;85:99-106.
9. Fernández-Formoso N, Rilo B, Mora MJ, Martínez-Silva I, Santana U. A paralleling technique modification to determine the bone crest level around dental implants. *Dentomaxillofac Radiol* 2011;40:385-389.

10. De Smet E, Jacobs R, Gijbels F, Naert I. The accuracy and reliability of radiographic methods for the assessment of marginal bone level around oral implants. *Dentomaxillofac Radiol* 2002;31:176-181.
11. Schulze RK, d'Hoedt B. Mathematical analysis of projection errors in "paralleling technique" with respect to implant geometry. *Clin Oral Implants Res* 2001;12:364-371.
12. Rugani P, Weingartner K, Jakse N. Influence of the Tube Angle on the Measurement Accuracy of Peri-Implant Bone Defects in Rectangular Intraoral X-ray Imaging. *J Clin Med* 2024;13.
13. Cosola S, Toti P, Peñarrocha-Diago M, Covani U, Brevi BC, Peñarrocha-Oltra D. Standardization of three-dimensional pose of cylindrical implants from intraoral radiographs: a preliminary study. *BMC Oral Health* 2021;21:100.
14. Afrashtehfar KI, Brägger U, Hicklin SP. Reliability of Interproximal Bone Height Measurements in Bone- and Tissue-Level Implants: A Methodological Study for Improved Calibration Purposes. *Int J Oral Maxillofac Implants* 2020;35:289-296.
15. Katafuchi M, Weinstein BF, Leroux BG, Chen YW, Daubert DM. Restoration contour is a risk indicator for peri-implantitis: A cross-sectional radiographic analysis. *J Clin Periodontol* 2018;45:225-232.
16. Yi Y, Koo KT, Schwarz F, Ben Amara H, Heo SJ. Association of prosthetic features and peri-implantitis: A cross-sectional study. *J Clin Periodontol* 2020;47:392-403.
17. Mattheos N, Janda M, Acharya A, Pekarski S, Larsson C. Impact of design elements of the implant supracrestal complex (ISC) on the risk of peri-implant mucositis and peri-implantitis: A critical review. *Clin Oral Implants Res* 2021;32 Suppl 21:181-202.
18. Janda M, Mattheos N. Prosthetic design and choice of components for maintenance of optimal peri-implant health: a comprehensive review. *Br Dent J* 2024;236:765-771.
19. Lops D, Meneghello R, Sbricoli L, Savio G, Bressan E, Stellini E. Precision of the Connection Between Implant and Standard or Computer-Aided Design/Computer-Aided Manufacturing Abutments: A Novel Evaluation Method. *Int J Oral Maxillofac Implants* 2018;33:23-30.

20. Han JW, Han JW, Pyo SW, Kim S. Impact of profile angle of CAD-CAM abutment on the marginal bone loss of implant-supported single-tooth posterior restorations. *J Prosthet Dent* 2023.
21. Nam JH, Chang J, Pyo SW, Kim S. The link between abutment configuration and marginal bone loss in subcrestally placed posterior implant-supported restorations. *J Prosthet Dent* 2025.
22. Yen JY, Hsu HJ, Lai YL, Chou IC, Chen YC, Lee SY. Efficacy of customized crown-level position jig in measuring peri-implant crestal bone level on periapical radiographs: An in vitro study. *J Dent Sci* 2024;19:338-344.
23. Sirin Y, Horasan S, Yaman D, et al. Detection of crestal radiolucencies around dental implants: an in vitro experimental study. *J Oral Maxillofac Surg* 2012;70:1540-1550.
24. Bonadiman EA, Fachetti EL, Haiter-Neto F, Pereira TCR, de-Azevedo-Vaz SL. Efficacy of a radiographic film holder adapter in generating radiographs of dental implants with improved geometric accuracy and sharpness. *J Prosthet Dent* 2024;132:419.e411-419.e417.
25. Darós P, Carneiro VC, Siqueira AP, de-Azevedo-Vaz SL. Diagnostic accuracy of 4 intraoral radiographic techniques for misfit detection at the implant abutment joint. *J Prosthet Dent* 2018;120:57-64.
26. French D, Grandin HM, Ofec R. Retrospective cohort study of 4,591 dental implants: Analysis of risk indicators for bone loss and prevalence of peri-implant mucositis and peri-implantitis. *J Periodontol* 2019;90:691-700.
27. Oh JH, Pyo SW, Chang JS, Kim S. Up to a 15-Year Survival Rate and Marginal Bone Resorption of 1780 Implants with or without Microthreads: A Multi Center Retrospective Study. *J Clin Med* 2023;12.
28. Benn DK. A review of the reliability of radiographic measurements in estimating alveolar bone changes. *J Clin Periodontol* 1990;17:14-21.

초록

치근단 방사선 사진에서 방사선 관구 각도와 디지털 센서 정렬이 CAD-CAM 지대주의 프로파일 각도 왜곡에 미치는 영향

목적: 본 연구는 CAD-CAM 맞춤형 지대주의 profile angle 을 치근단 방사선 사진으로 측정할 때, 방사선 관구의 수직 회전, 수평 회전 및 디지털 센서의 수평 회전이 측정값에 미치는 영향을 평가하고자 하였다. 또한 임플란트가 치조제에서 협측 또는 설측으로 편심되게 위치하는 경우, 방사선 영상의 왜곡 정도에 영향을 주는지를 확인하였다.

재료 및 방법: 중심, 협측 및 설측으로 1.0 mm, 1.5 mm 오프셋된 5 개의 임플란트 위치를 모형에 설정하였고, 표준화된 CAD-CAM 지대주 및 단일 도재관을 제작하였다. 방사선 촬영은 수직 관구 각도(0°–20°), 수평 관구 각도(근심/원심 방향 0°–20°), 수평 센서 회전각(0°–20°) 조건에서 시행되었으며, interthread distance 및 근심/원심 profile angle 을 측정하여 STL 기준값과 비교하였다. 인접치와의 보철물 중첩도 또한 분석하였다.

결과: 수직 관구 회전이 15°를 초과하거나 센서 회전이 10°를 초과하는 경우, interthread 거리와 profile angle 에 유의한 왜곡이 발생하였다. 수평 관구 회전은 특히 협측에 위치한 임플란트에서 근·원심 방향으로 비대칭적인 왜곡을 초래하였다. Interthread distance 왜곡이 10% 이상이거나 보철물 중첩이 10% 이상인 경우, profile angle 의 측정 오차가 5°를 초과하는 경향이 나타났다.

결론: CAD-CAM 지대주의 profile angle 측정은 방사선 투영각도의 미세한 변화에도 민감하게 반응한다. 정확한 측정을 위해서는 방사선 관구와 센서의 정렬을 임플란트 장축에 수직으로 유지하고, 인접치와의 중첩을 최소화하는 촬영이 요구된다. Interthread distance 및 crown overlap 은 영상 신뢰도를 판단할 수 있는 간접적 지표로 활용될 수 있다. 본 연구 결과는 향후 임상적 적용과 자동화된 영상 분석 시스템 개발의 기초자료로 활용될 수 있다.

주제어: 프로파일 앵글, CAD-CAM 맞춤형 지대주, 치근단 방사선, 방사선 관구 회전량, 디지털 센서 회전량